Annals of Diagnostic Pathology 41 (2019) 96–101

Contents lists available at ScienceDirect

Annals of Diagnostic Pathology

journal homepage: www.elsevier.com/locate/anndiagpath

Original Contribution

Clear cell renal cell carcinoma with Paneth-like cells: Clinicopathologic, morphologic, immunohistochemical, ultrastructural, and molecular analysis of 13 cases☆

Fumiyoshi Kojima[a], Stela Bulimbasic[b], Reza Alaghehbandan[c], Petr Martinek[d], Tomas Vanecek[d], Kvetoslava Michalova[d], Kristyna Pivovarcikova[d], Michal Michal[d], Milan Hora[e], Shin-ichi Murata[a], Emiko Sugawara[f], Joanna Rogala[d], Rinë Limani[g], Ondrej Hes[d,*]

[a] Department of Human Pathology, Wakayama Medical University, Wakayama, Japan
[b] Clinical Department of Pathology and Cytology, University Hospital Centre Zagreb, Croatia
[c] Department of Pathology, Faculty of Medicine, University of British Columbia, Royal Columbian Hospital, Vancouver, BC, Canada
[d] Department of Pathology, Charles University in Prague, Faculty of Medicine in Plzeň, Pilsen, Czech Republic
[e] Department of Urology, Charles University in Prague, Faculty of Medicine in Plzeň, Pilsen, Czech Republic
[f] Department of Pathology, Musashino Red Cross Hospital, Tokyo, Japan
[g] Institute of Pathology, Hospital and University Clinic Services of Kosovo, Prishtina, Kosovo

ARTICLE INFO

Keywords:
Kidney
Clear cell renal cell carcinoma
Paneth-like cells
Immunohistochemistry
Next generation sequencing

ABSTRACT

Clear cell renal cell carcinoma (CRCC) is well known for its intratumoral heterogeneity. Paneth-like cells (PLC) have been reported in variable organs (i.e., hepatobiliary, genitourinary, and female genital tract). In genitourinary system, it is possible to find PLCs in epididymis, urinary bladder and prostate. The objective of this study was to assess PLC in CRCCs 13 CRCCs with prominent PLC (CRCCPLC) were selected out of 1378 CRCCs in our registry. The tumors were analyzed using morphologic, immunohistochemical, ultrastructural, and molecular genetic methods.

CRCCPLCs were mostly of low histologic grade (12/13). Immunohistochemical profile was compatible with classic CRCC. PLC constituted 10 to–70% of the tumor volume (mean 17.7%, median 10%). PLCs did not express neuroendocrine markers (chromogranin, synaptophysin, CD56, INSM-1). Ultrastructurally, PLCs were filled by membrane bounded vesicles of various sizes and were compatible with secretory type of cells. *VHL* mutation was found in 9/9 cases, and LOH3p was found in 6/8 analyzable cases.

Conclusions: PLC morphology can variably be present in "classic" CRCC, even in a substantial proportion. Ultrastructurally, PLCs have all attributes of secretory cells. Preliminary follow up data showed that these tumors may not be associated with aggressive clinical behavior.

1. Introduction

Intratumor heterogeneity (ITH) is a well-established phenomenon in carcinogenesis extensively studied in many neoplasms including the genitourinary system. While intertumor heterogeneity is a well-known event in renal cell carcinomas (RCCs), ITH has been overlooked by urological pathologists for years. ITH of RCC was already demonstrated back in 1988 [1]. In routine practice, ITH in renal tumors can cause diagnostic discrepancies between core biopsy and resection specimens which could have prognostic/therapeutic implications, i.e. possible failure of targeted therapy [2]. In situation, when the tumor is insufficiently sampled, ITH may also be responsible for unpredictable aggressive clinical behavior that some RCCs display [2].

Paneth cells are located in normal mucosa of the duodenum and small intestine where they serve as a part of antimicrobial barrier of the gastrointestinal tract [3]. They can also be encountered in large bowel affected by chronic inflammatory processes [4]. Paneth-like cells (PLC), which are different from genuine Paneth cells, are cells with

☆ This study was supported by the Charles University Research Fund (project number Q39) and by the grant of Ministry of Health of the Czech republic-Conceptual Development of Research Organization (Faculty Hospital in Plzen- FNPl 00669806).

* Corresponding author at: Department of Pathology, Charles University, Medical Faculty and Charles University Hospital Plzen, Alej Svobody 80, 304 60 Pilsen, Czech Republic.
E-mail address: hes@medima.cz (O. Hes).

https://doi.org/10.1016/j.anndiagpath.2019.05.012

voluminous cytoplasm packed with eosinophilic granules [5]. PLCs have been reported in different organs including hepatobiliary tract, genitourinary system, and female genital tract [6-13]. Within the genitourinary system, PLCs occasionally occur in normal epididymis [8,9] or as a component of urinary bladder and prostate tumors [13,14]. With respect to renal tumors, presence of PLC is rarely mentioned in the literature [10]. In our experience, clear cell renal cell carcinoma (CRCC) can demonstrate scattered, easily overlooked PLCs. We assembled a cohort of 13 cases, where PLCs were prominent and conspicuous. The aim of this study was to characterize CRCC with prominent PLCs (CRCCPLC) using morphologic, immunohistochemical, ultrastructural, and molecular genetic methods.

2. Materials and methods

2.1. Study design

Of approximately 26,000 renal tumors and tumor-like renal lesions in the Plzen Tumor Registry, 1378 cases of CRCC were retrieved. Thirteen CRCCPLCs were subsequently selected for study.

2.2. Histological analyses

The tissues were fixed in neutral formalin, embedded in paraffin, cut into 2–4 μm thin sections and stained with Hematoxylin and Eosin (H& E). One to nine paraffin blocks were available for each case. All tumors were independently reviewed by two pathologists (FK and OH). Clinicopathologic and follow-up data were collected using medical records available from each participating institution.

2.3. Immunohistochemical analyses

The immunohistochemical study was performed using a Ventana Benchmark XT automated immunostainer (Ventana Medical System, Inc., Tucson, AZ, USA) on formalin fixed, paraffin embedded (FFPE) tissue. The following primary antibodies were employed: CK7 (OV-TL12/30, monoclonal, DakoCytomation, Glostrup, Denmark, 1:200), alpha-methylacyl-CoA-racemase (AMACR) (P504S, monoclonal, Zeta, Sierra Madre, CA, 1:50), vimentin (D9, monoclonal, NeoMarkers, Westinghouse, CA, 1:1000), Melan A (A103, monoclonal, Ventana, RTU), antimitochondrial antibody (MIA) (113–1, monoclonal, Biogenex, San Ramon, CA, 1:500), carbonic anhydrase IX (CAIX) (rhCA9, monoclonal, RD systems, Abingdon, GB, 1:100), CD10 (monoclonal 56C6, Leica, Newcastle, UK, 1:20), CD56 (1B6, monoclonal, Leica Biosystems, Newcastle, UK, 1:100), synaptophysin (polyclonal, LabVision, Fremont, CA, 1:350), chromogranin A (monoclonal, DAK-A3, DakoCytomation, 1:600), ISMN-1 (monoclonal, A-8, Santa Cruz, US, 1:1000). The primary antibodies were visualized using a supersensitive streptavidin-biotin-peroxidase complex (BioGenex). Internal biotin was blocked by standard protocol used by Ventana Benchmark XT automated stainer (hydrogene peroxide based). Appropriate positive and negative controls were employed. We regarded the result as positive findings if the intensity was more than mild, and evaluated the proportional score as follows: 0 negative, focal $< 50\%$; diffuse $\geq 50\%$.

2.4. Ultrastructural analyses

Electron microscopy evaluation was performed on five cases. Small pieces of paraffin-embedded tumor tissue with Paneth-like changes from 5 cases (No 3, 6, 8, 12, and 13) were de-paraffinized and further routinely processed for ultrastructural analysis. Semi-thin sections of epoxy embedded tissue were stained with toluidine blue and examined by light microscopy. Ultrathin sections from representative area were cut, stained with uranyl acetate and lead citrate, and examined with a JEOL (Tokyo, Japan) JEM 1400 Transmission Electronic Microscope using Olympus iTEM universal TEM imaging platform.

2.5. Molecular analyses

2.5.1. Mutational analyses

Sanger sequencing and methylation of *VHL* gene, and analysis of loss of heterozygosity (LOH) of locus 3p were performed using previously described methods [15].

2.5.2. Targeted next-generation sequencing

A panel of 271 cancer related genes (Comprehensive cancer panel, Qiagen, Hilden, Germany) were used to analyze tumor tissue samples. The samples were isolated using macro dissection from FFPE blocks. DNA was isolated using Qiagen DNA mini kit, and 250 ng of DNA was used to construct the library. Library was sequenced on Illumina's Nextseq 500, aiming at average coverage 350 x after deduplication of molecular barcodes to detect 10% allele frequency with 95% sensitivity. Variants were called using Qiagen's proprietary pipeline. Subsequently the variants were filtered using the calculated limit of detection for each sample. Furthermore the variants were annotated using The Genome Aggregation Database (GnomAD) [16] for population statistics and ClinVar database [17] or the relationships among variations and phenotypes. Variants more frequent than 1% in the GnomAD database were excluded as well as known benign variants according to the ClinVar database. The remaining subset was checked visually and suspected artefactual variants were excluded.

3. Results

3.1. Clinicopathological findings

Basic clinicopathologic data are summarized in Table 1. The patients were 10 males and 2 females, with age ranged from 25 to 74 years (median 61, mean 55.1). Detailed clinicopathologic data for one patient were not available. The tumor size ranged from 1.2 to 8.5 cm (mean 3.6). Eight patients were pT1a, 3 were pT1b, and 1 was pT2a according to TNM staging (8th edition of AJCC). Grossly, the tumors were mostly solid, yellow to tan, with occasionally foci of regressive changes or hemorrhage. Follow up data were available for 10 patients, ranged from 0.5 to 11 years. No metastatic disease or any clinical aggressive behavior was identified in any case. However, one patient with confirmed VHL syndrome had anamnesis of multiple CCRCCs (without PLC), and another patient underwent renal resection of contralateral CCRCC, 3 years prior to the current surgery (detailed information present in Table 1).

Microscopically, all CRCCPLCs were well-circumscribed, occasionally encircled by fibrous pseudocapsule. Tumors were arranged in mixed solid-alveolar, tubular, or cystic growth patterns. In two cases, prominent regressive changes were encountered. Tubular or cystic structures filled with eosinophilic proteinaceous fluid were prominent in 8 cases. Necrosis or lymphovascular invasion were not seen. All but one case showed low-grade histology (grade 1 or 2– according Fuhrman/ISUP grading system). PLCs were arranged in groups, formed conspicuous bright red areas (Fig. 1). Groups of PLC formed solid foci or lined tubular or pseudotubular structures (Fig. 2). Larger tubules had cystic appearance with prominent PLC lining (Fig. 3A and B). PLCs were large with cytoplasmic eosinophilic round granules (Fig. 4). Granules positively stained with diastase digestive Periodic-Schiff stain (d-PAS) with maximum intensity in the apical part of the cells.

Immunohistochemical findings are summarized in Table 2. Most CRCCPLCs were positive for vimentin, CAIX, CD10, AMACR, and MIA. Six of 13 CRCCPLCs showed focal positivity for CK7. All CRCCPLCs were negative for neuroendocrine (NE) markers, namely ISMN-1, chromogranin A, synaptophysin, and CD56.

Table 1
Clinicopathological findings of CRCCPLCs.

Case	Age	Sex	Tumor size[b] (cm)	Stage	Follow up (years)	PLCs (%)	Necrosis	LVI	ISUP	Growth pattern
1	61	m	3.0	1a	1AW	30	0	0	2	Tubular
2	71	m	8.5[b]	2a	LFU	20	0	0	3	Solid-tubular
3	65	f	4.5	1b	5AW	10	0	0	2	Solid alveolar
4	25	m	1.2	1a	2AW	10	0	0	2	Tubulocystic
5	NA	NA	NA	NA	NA	20	0	0	2	Solid-tubular
6	35	m	3.2	1a	11AW[c]	10	0	0	1	Tubulocystic
7	47	m	3	1a	5AW[d]	10	0	0	2	Solid alveolar
8	67	f	1.2	1a	4AW	10	0	0	2	Solid-tubular
9	62	m	6.5	1b	3AW	10	0	0	1	Solid alveolar with cyst
10	74	m	1.8	1a	LFU	10	0	0	1	Solid alveolar
11	49	m	5.5	1b	3AW	10	0	0	1	Tubular
12[a]	61	m	2.5	1a	3AW	10	0	0	2	Solid alveolar
13	44	m	2.5	1a	0.5 AW	70	0	0	2	Tubular

Abbreviation; NA, not available; m, male; f, female; AW, alive without disease; LE,; PLCs, Paneth-like cells; LVI, lymphovascular invasion; LFU, lost to follow up; ISUP, Fuhrman/ISUP grade.

[a] Von Hippel Lindau syndrome and multifocal tumor.
[b] Maximum diameter.
[c] Basalioma of chest and lipoma of the tight 8 years after nephrectomy.
[d] 3 years prior current surgery, contralateral resection of low grade clear cell renal cell carcinoma without Paneth-like cells.

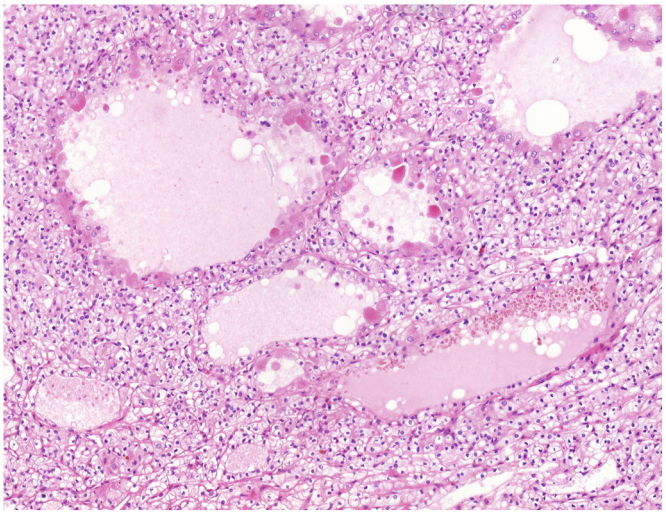

Fig. 1. PLCs were arranged in groups or tubules and formed conspicuous bright red areas. (For interpretation of the references to color in this figure legend, the reader is referred to the web version of this article.)

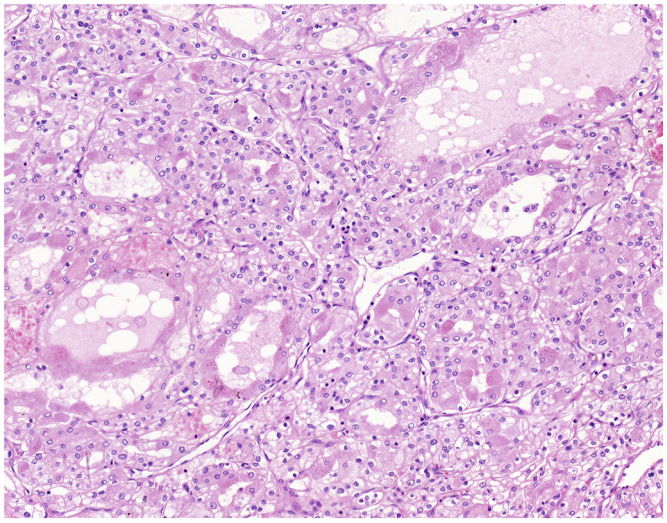

Fig. 2. Clear cell population is visible on the background with prominent PLCs growing in solid and tubular pattern.

3.2. Electron microscopical findings

Ultrastructural analysis revealed moderately preserved tumor tissue composed of large polygonal cells organized in solid nests and lining microcystic spaces. There were two types of cells with the first one type showing typical features of CRCC, i.e., abundant clear cytoplasm and irregular nuclei with occasional prominent nucleoli. Lipid droplets were dissolved during processing for light microscopy, leaving large pale spaces without other cytoplasmic structures. The second cell type, corresponding to PLCs seen on light microscopy, showed moderate amount of large cytoplasmic secretory granules, ranging from 1.45 to 2.85 μm in diameters (Fig. 5). Some of the granules were dispersed through cytoplasm, others located in upper, luminal part of the cell. Typical electron dense NE type granules, larger amount of glycogen particles or other specific structures were not found.

3.3. Molecular genetic findings

Eleven CRCCPLCs were selected for molecular genetic testing, of which nine samples were analyzable. The results of genetic analyses are shown in Table 3. The NGS sequencing of the mutation panel was successful in six cases; two cases did not meet the expected sequencing quality control and were reported as not analyzable. A total of 47 variants were found including variants in genes *ROS1* and *LRP1B* appearing more in two cases. The number of mutations per each case ranged from 1 to 16 (mean 7.83, median 6). In three cases with insufficient DNA quality for NGS, we performed Sanger sequencing of *VHL* gene, and further performed LOH analysis of chromosome locus 3p. Together we detected 9 *VHL* mutations and 6 LOH of locus 3p. No hypermethylation status of *VHL* promoter was detected in eight successfully analyzed cases. Two cases were not included in the molecular genetic studies due to insufficient amount of tissue material.

4. Discussion

CRCC is well-known for its high ITH. The spectrum of ITH is a broad, encompassing uniform CRCCs together with considerably morphologically and architecturally heterogenous cases [2,18]. It has been shown that ITH is an inherent process of tumorigenesis and it seems that it has become a major obstacle for the successful targeted therapy [19]. Hence, gross description and extensive sampling play a crucial role in the examination of CRCC. Multisite tumor sampling enhances

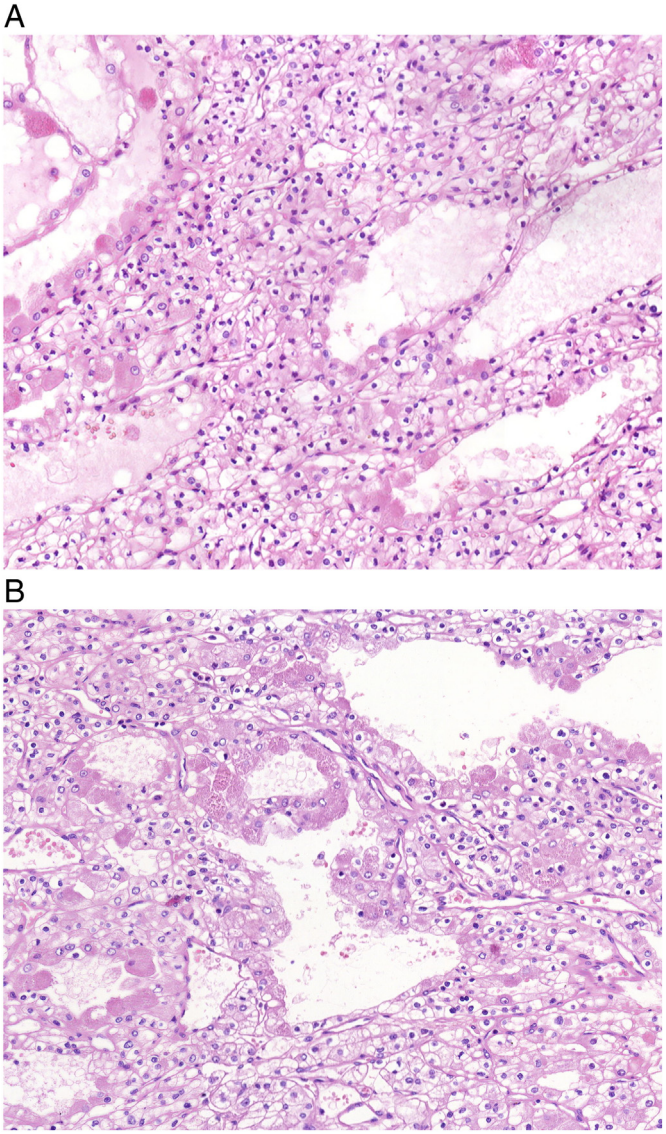

Fig. 3. PLCs formed cell lining of smaller cysts (A). Pseudostratification was noted in some cystic spaces (B).

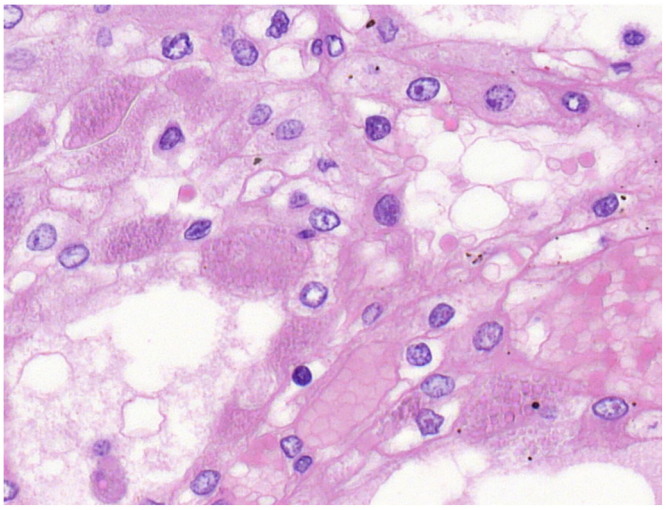

Fig. 4. PLCs were large cells with voluminous cytoplasm filled by intracytoplasmic eosinophilic round granules.

the detection of ITH at all different temporal stages of tumor evolution [20,21]. In this study we focused on CRCCs with unusual cytologic features represented by prominent voluminous neoplastic cells filled by fine eosinophilic droplets. Such cells remarkably resembled Paneth cells of the gastrointestinal tract. To the best of our knowledge, the presence of prominent and conspicuous PLC is to date undocumented phenomenon in CRCC. Genuine Paneth cells are considered as fully differentiated cell, located in the deep portion of a crypt in mucosa of gastrointestinal tract. Paneth cells contain defensin, lysozyme and phospholipase A2 within their cytoplasm [3]. Histochemically, the granules within Paneth cells are positive for PAS stain with or without diastase digestion as well as a1-antitrypsin [22]. Some reports documented that so-called intestinal type adenocarcinoma of urinary bladder, uterine cervix, ovary, and gallbladder may also contain Paneth cells [6,7,11,12]. Based on their almost identical appearance to intestinal adenocarcinoma, we supposed they are closely related to those in the small intestine.

The situation of Paneth cells in the prostate is different. It has been shown that cells resembling Paneth cells within prostatic adenocarcinoma contained NE granules [23]. Those cells were smaller and more uniform than PLCs documented in our series. Moreover, NE granules were mostly located in the sub-nuclear portion of the cell, similarly to genuine endocrine cells in the gastrointestinal tract. Interestingly, prostatic adenocarcinoma with Paneth cell-like NE differentiation has been reported to have a better prognosis than conventional acinar adenocarcinoma, equally graded as Gleason pattern 5 [24,25]. PLCs were morphologically and immunohistochemically distinct from NE cells and the tumors in our series did not show any apparent features of NE differentiation.

PLCs within CRCC were first reported by Krishnan and Truong in 2002 [10]. However, their study was focused on ultrastructure and no data about clinical, morphological, immunohistochemical, and molecular genetic features were provided. Most of our cases had tubular and cystic structure, and were morphologically compatible with classic CRCC. All but one case were low stage and low grade tumors. Based on our ultrastructural finding, it seems that granules within PLC were secretory granules. This finding is different from what Krishan and Truong concluded that granules in their cases were lysosomes. It is possible that Paneth-like granule is formed by variable constituents.

Besides PLC, another type of membrane bounding particles were described. So-called glassy hyaline globules occur in CRCC and some papillary RCCs. These globules are different in many aspects from granules found in PLCs [26]. Glassy hyaline globules are encountered mostly in tumors with high grade features (so-called “granular variant” of CRCC) and are located predominantly extracellularly. On the contrary, PLC in the current study were part of the low-grade tumors and were located exclusively in intracellular space. Another type of globules, so-called rhabdoid globules, was described within renal oncocytoma. Gatalica and Guarino documented such globules mainly in renal oncocytoma and in some RCCs (clear cell RCC, chromophobe RCC, or papillary RCC) [27,28]. Based on immunohistochemical and ultrastructural examinations, they suggested these globules were derived from basement membrane. The globules documented in renal oncocytoma were quite different from those of PLCs on the following points: location (extra vs intracytoplasmic), number (sparse vs frequent), size (large vs small in diameter), and shape (round vs lobulated).

Out of the kidneys, epididymis is another genitourinary organ where PLCs were described. In epididymis, the morphology of PLCs was similar to that documented by Krishnan and Truong in CRCC. Epididymal PLCs were filled with lysosomes [10]. Nistal et al. reported epididymal PLCs were positive for a1-antichymotrypsin and CD68, contrary to intestinal Paneth cells [9]. Shah et al. suggested a possible relationship between the presence of PLCs and epididymal obstruction [8]. Nistal et al. reported 9 cases of epididymis with prominent PLCs, co-occurring with testicular tumor without evidence of epididymal

Table 2
Immunohistochemical findings of CRCCPLCs.

Case	Vimentin	CA9	CD10	CK7	AMACR	ISMN1	Chromogranin a	Synaptophysin	CD56	MIA
1	f	f	d	f	d	0	0	0[a]	0[a]	d
2	f	d	d	0	d	0	0	0[a]	0[a]	d
3	f	d	d	0	f	0	0	0	0	d
4	d	d	d	f	d	0	0	0[a]	0[a]	d
5	d	0	d	d	d	0	0	0	0	d
6	d	d	f	d	d	0	0	0	0[a]	d
7	d	d	d	d	d	0	0	0	0	d
8	d	d	d	d	d	0	0	0[a]	0[a]	d
9	d	0	f	0	f	0	0	0	0	0
10	d	d	d	0	d	0	0	0	0	f
11	d	0	d	0	0	0	0	0[a]	0[a]	f
12	d	0	f	0	d	0	0	0	0	f
13	d	f	d	0	d	0	0	0	0	d

Abbreviation; f, focal; d, diffuse.
[a] Non-specific cytoplasmic granular staining.

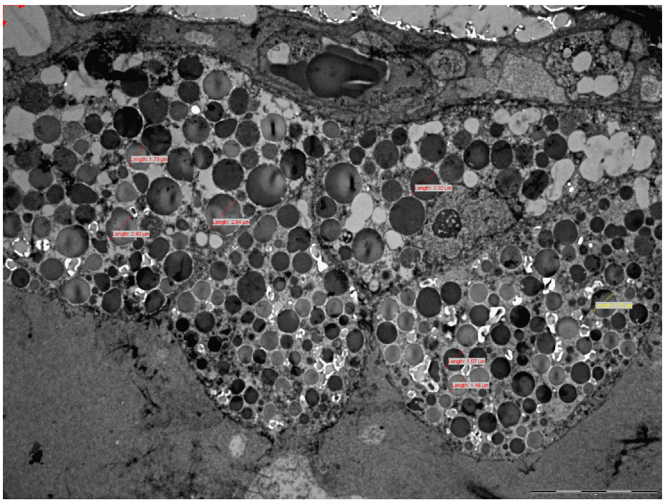

Fig. 5. PLCs showed moderate amount of large cytoplasmic secretory granules, ranging from 1.45 to 2.85 μm in diameters.

obstruction. They postulated that increase of endocytolytic activity for intraluminal fluid storage lead to formation of PLCs. CRCCPLCs in our series composed of dilated tubules or cystic structures containing eosinophilic fluid with PLCs distributed around such regions. These findings supported the theory of Nistal, et al. that excess fluid lead to formation of PLC.

As indicated earlier, all cases included in this study containing prominent areas of PLCs were low-grade. However, single PLC or small inconspicuous groups of PLCs can also be present in CRCCs with high grade morphologic features (grade 3 and 4). Such tumors characteristically show marked ITH and the distribution of PLCs is mainly in the low grade areas.

All 9 presented CRCCPLCs had *VHL* mutation and 6 had also LOH 3p, which are characteristic genetic features for CRCC. We found multiple mutations in other tested genes, only two genes (*ROS1, LRP1B*) were found mutated in two different cases. This does not significantly differ from the findings of combined studies of CRCCs that showed mutations in these genes to be present in 3.2 and 2.7%, respectively (datasets of 502 tested samples available via the cBioPortal) [29]. Since most of the gene mutations presented herein have already been reported in CRCC, we consider molecular features of CRCCPLCs compatible with the diagnosis of CRCC. Hypermethylation of VHL promoter was not found in the analyzed cases, which is consistent with the reported hypermethylation of 7% CRCC found in the Cancer Genome Atlas Research Network studies [30].

In the differential diagnosis, particularly in limited material (core biopsy), Xp11.2 translocation RCC should be considered. The morphology of Xp11.2 translocation RCCs can be variable, depending on many factors including fusion partner [31]. Translocation Xp11.2 RCC should be always considered within the differential diagnosis in case of tumor composed of clear cells mixed with voluminous eosinophilic cells. However, in our cases there were no psammoma bodies, prominent microcalcifications, papillary structures or fully developed papillae. Also, the vasculature was prominent in our cases, as it is characteristic for CRCC rather than for Xp11.2 translocation RCCs. In difficult cases an immunohistochemical panel (together with FISH) can

Table 3
Molecular genetic findings of CRCCPLCs.

Case #	HCCP	LOH3p	*VHL* methylation	*VHL* Sanger	*VHL* mutation
1	NP	NP	NP	NP	
2	8	+	−	NP	c.419del p.(Leu140ProfsTer19)
3	NP	+	−	+	c.256C > A p.(Pro86Thr)
4	1	−	−	NP	c.233A > T p.(Asn78Ile)
5	NP	NP	NP	NP	
6	4	+	−	NP	c.302 T > G p.(Leu101Arg)
7	4	+	−	NP	c.341-2dup p(?)
8	14	NP	NP	NP	c.563 T > A p.(Leu188Gln)
9	NP	NA	NA	NA	
10	NP	NA	NA	NA	
11	NA	+	−	+	c.296_333dup p.(Tyr112GlnfsTer60)
12	NA	+	−	+	c.349 T > C p.(Trp117Arg)
13	16	−	−	NP	c.611_612del p.(Glu204AlafsTer51)

Abbreviation; NA not analyzable, NP not performed, + positive, − negative, HCCP – Human Comprehensive Cancer NGS panel (with number of detected variants), LOH3p – loss of heterozygosity of chromosome 3p, *VHL* Sanger – Sanger sequencing of *VHL* gene.

aid in arriving at the accurate diagnosis. Metastatic carcinoma should also be included in the differential diagnosis.

In conclusion, we found that CRCCPLC do not have distinct clinical, immunohistochemical, and genetic features and that they are part of morphologic spectrum of usual low grade CRCC. The prognosis does not seem to be affected by the presence or absence of PLCs.

Declaration of Competing Interest

All authors declare no conflict of interest.

References

[1] Nordenson I, Ljungberg B, Roos G. Chromosomes in renal carcinoma with reference to intratumor heterogeneity. Cancer Genet Cytogenet 1988;32(1):35–41.
[2] Zaldumbide L, Erramuzpe A, Guarch R, Cortes JM, Lopez JI. Large (> 3.8 cm) clear cell renal cell carcinomas are morphologically and immunohistochemically heterogeneous. Virchows Arch 2015;466(1):61–6.
[3] Bevins CL, Salzman NH. Paneth cells, antimicrobial peptides and maintenance of intestinal homeostasis. Nat Rev Microbiol 2011;9(5):356–68.
[4] Tanaka M, Saito H, Kusumi T, Fukuda S, Shimoyama T, Sasaki Y, et al. Spatial distribution and histogenesis of colorectal Paneth cell metaplasia in idiopathic inflammatory bowel disease. J Gastroenterol Hepatol 2001;16(12):1353–9.
[5] Nevalainen TJ, Shah VI, de Peralta-Venturina M, Amin MB. Absence of group II phospholipase A2, a Paneth cell marker, from the epididymis. APMIS 2001;109(4):295–8.
[6] Albores-Saavedra J, Nadji M, Henson DE. Intestinal-type adenocarcinoma of the gallbladder. A clinicopathologic study of seven cases. Am J Surg Pathol 1986;10(1):19–25.
[7] Pallesen G. Neoplastic Paneth cells in adenocarcinoma of the urinary bladder: a first case report. Cancer 1981;47(7):1834–7.
[8] Shah VI, Ro JY, Amin MB, Mullick S, Nazeer T, Ayala AG. Histologic variations in the epididymis: findings in 167 orchiectomy specimens. Am J Surg Pathol 1998;22(8):990–6.
[9] Nistal M, Marino-Enriquez A, De Miguel MP. Granular changes (Paneth cell-like) in epididymal epithelial cells are lysosomal in nature and are not markers of obstruction. Histopathology 2007;50(7):944–7.
[10] Krishnan B, Truong LD. Renal epithelial neoplasms: the diagnostic implications of electron microscopic study in 55 cases. Hum Pathol 2002;33(1):68–79.
[11] Lee KR, Trainer TD. Adenocarcinoma of the uterine cervix of small intestinal type containing numerous Paneth cells. Arch Pathol Lab Med 1990;114(7):731–3.
[12] Bigelow B, Blaustein A. Paneth cells in a mucinous cystadenoma of the ovary: light and electron microscopic study. Gynecol Oncol 1978;6(4):391–4.
[13] Weaver MG, Abdul-Karim FW, Srigley J, Bostwick DG, Ro JY, Ayala AG. Paneth cell-like change of the prostate gland. A histological, immunohistochemical, and electron microscopic study. Am J Surg Pathol 1992;16(1):62–8.
[14] Chen YB, Epstein JI. Primary carcinoid tumors of the urinary bladder and prostatic urethra: a clinicopathologic study of 6 cases. Am J Surg Pathol 2011;35(3):442–6.
[15] Petersson F, Grossmann P, Hora M, Sperga M, Montiel DP, Martinek P, et al. Renal cell carcinoma with areas mimicking renal angiomyoadenomatous tumor/clear cell papillary renal cell carcinoma. Hum Pathol 2013;44(7):1412–20.
[16] Lek M, Karczewski KJ, Minikel EV, Samocha KE, Banks E, Fennell T, et al. Analysis of protein-coding genetic variation in 60,706 humans. Nature 2016;536(7616):285–91.
[17] Landrum MJ, Lee JM, Benson M, Brown GR, Chao C, Chitipiralla S, et al. ClinVar: improving access to variant interpretations and supporting evidence. Nucleic Acids Res 2018;46(D1). [D1062-D7].
[18] Lopez JI. Intratumor heterogeneity in clear cell renal cell carcinoma: a review for the practicing pathologist. APMIS 2016;124(3):153–9.
[19] Erramuzpe A, Cortes JM, Lopez JI. Multisite tumor sampling enhances the detection of intratumor heterogeneity at all different temporal stages of tumor evolution. Virchows Arch 2018;472(2):187–94.
[20] Lopez JI, Cortes JM. Multisite tumor sampling: a new tumor selection method to enhance intratumor heterogeneity detection. Hum Pathol 2017;64:1–6.
[21] Lopez JI, De Petris G. Discovering intratumor heterogeneity: the next frontier for pathologists. Pathologica 2017;109(2):110–3.
[22] Molmenti EP, Perlmutter DH, Rubin DC. Cell-specific expression of alpha 1-antitrypsin in human intestinal epithelium. J Clin Invest 1993;92(4):2022–34.
[23] Epstein JI, Amin MB, Beltran H, Lotan TL, Mosquera JM, Reuter VE, et al. Proposed morphologic classification of prostate cancer with neuroendocrine differentiation. Am J Surg Pathol 2014;38(6):756–67.
[24] Tamas EF, Epstein JI. Prognostic significance of paneth cell-like neuroendocrine differentiation in adenocarcinoma of the prostate. Am J Surg Pathol 2006;30(8):980–5.
[25] So JS, Gordetsky J, Epstein JI. Variant of prostatic adenocarcinoma with Paneth cell-like neuroendocrine differentiation readily misdiagnosed as Gleason pattern 5. Hum Pathol 2014;45(12):2388–93.
[26] Hes O, Michal M, Sulc M, Kocova L, Hora M, Rousarova M. Glassy hyaline globules in granular cell carcinoma, chromophobe cell carcinoma, and oncocytoma of the kidney. Ann Diagn Pathol 1998;2(1):12–8.
[27] Guarino M, Zuccoli E, Garda E, Cristofori E, Pallotti F, Nebuloni M, et al. Extracellular matrix globules in renal oncocytoma. Pathol Res Pract 2001;197(4). [245–52].
[28] Gatalica Z, Miettinen M, Kovatich A, McCue PA. Hyaline globules in renal cell carcinomas and oncocytomas. Hum Pathol 1997;28(4). [400–3e].
[29] Cerami E, Gao J, Dogrusoz U, Gross BE, Sumer SO, Aksoy BA, et al. The cBio cancer genomics portal: an open platform for exploring multidimensional cancer genomics data. Cancer Discov 2012;2(5):401–4.
[30] Comprehensive molecular characterization of clear cell renal cell carcinoma. Nature 2013;499(7456):43–9.
[31] Argani P, Zhong M, Reuter VE, Fallon JT, Epstein JI, Netto GJ, et al. TFE3-fusion variant analysis defines specific Clinicopathologic associations among Xp11 translocation cancers. Am J Surg Pathol 2016;40(6):723–37.